Pressure correction in density-functional calculations

Shun Hang Lee* and Jones Tsz Kai Wan†
Department of Physics, The Chinese University of Hong Kong, Shatin, New Territories, Hong Kong.
(Dated: November 11, 2008)

First-principles calculations based on density functional theory have been widely used in studies of the structural, thermoelastic, rheological, and electronic properties of earth-forming materials. The exchange-correlation term, however, is implemented based on various approximations, and this is believed to be the main reason for discrepancies between experiments and theoretical predictions. In this work, by using periclase MgO as a prototype system we examine the discrepancies in pressure and Kohn-Sham energy that are due to the choice of the exchange-correlation functional. For instance, we choose local density approximation and generalized gradient approximation. We perform extensive first-principles calculations at various temperatures and volumes and find that the exchange-correlation-based discrepancies in Kohn-Sham energy and pressure should be independent of temperature. This implies that the physical quantities, such as the equation of states, heat capacity, and the Grüneisen parameter, estimated by a particular choice of exchange-correlation functional can easily be transformed into those estimated by another exchange-correlation functional. Our findings may be helpful in providing useful constraints on mineral properties at deep Earth thermodynamic conditions.

Keywords: pressure correction, density functional theory, exchange-correlation, Car-Parrinello molecular dynamics.

I. INTRODUCTION

In recent decades, first-principles (FP) calculations with density functional theory (DFT) [1, 2] have been widely adopted in studies of the structural, thermoelastic, rheological, and electronic properties of materials, molecules, and minerals in research areas that range from physics and chemistry to biology and geosciences [3, 4, 5, 6, 7, 8]. The modern implementation of FP techniques is based on different approximations, such as the pseudopotential (PP) method, the expansion of electronic wavefunctions by modal functions, and the choice of exchange-correlation (XC) functionals. As a result, the predictions made by different FP calculations may differ from one another moderately.

Many techniques have been developed to enhance the accuracy and efficiency of FP calculations. Examples include the projector-augmented wave (PAW) method [9], and maximally localized Wannier functions [10]. However, due to inadequate knowledge, the exact form of exchange-correlation functional remains unknown and the search for a precise XC term has been an active area of research. The choice of XC in FP calculations has been shown to be the main reason for the inconsistencies between these various calculations [11, 12, 13, 14, 15, 16]. In particular, the pressures calculated by generalized gradient approximation (GGA) [17] and local density approximation (LDA) [18] are known to be systematically over- and underestimated, and a common way to choose the XC functional is to use the XC that gives the best agreement with experiments.

In this article, we investigate the way in which such a pressure difference depends on volume and temperature. If this difference can be quantified, simulations can be performed using either exchange-correlation, and at the same time, obtaining the results of the other. This would be an efficient way of constraining the thermodynamic quantities. For example, Karki et al. [11] calculated the elastic properties of $MgSiO_3$ at pressures up to the lower mantle condition using LDA, which gave an equilibrium volume and elastic constant consistent with experiments [19, 20]. However, calculations by Oganov et al. [13, 14] on $MgSiO_3$ have shown that the GGA gives an extremely accurate elastic constant and the volume dependencies of the elastic properties, although the pressure is overestimated. The authors thus applied a constant pressure shift to the equation of state (EOS) estimated by GGA and then matched the measured ambient pressure EOS, which resulted in an excellent match between the experimental observations and the FP calculation results.

II. THEORY

To quantify the relationship between the pressure difference and the XC functionals, we first consider the total internal energy of a system, which is contributed by the interaction energy between particles and the total kinetic energy of the ions and electrons. At thermal equilibrium, this total internal energy is given by

$$U = \Big\langle \sum_I \frac{1}{2} M_I \dot{R}_I^2 \Big\rangle + \Big\langle \sum_{I,J\neq I} \frac{1}{2} \frac{q_I q_J}{|\mathbf{R}_I - \mathbf{R}_J|} \Big\rangle + \Big\langle E_{\rm KS}[\{\mathbf{R}_I\}, \{\psi_n\}] \Big\rangle, \quad (1)$$

where $\langle \cdots \rangle$ denotes the ensemble average, and $\{\mathbf{R}_I\}$ and $\{\psi_n\}$ represent ionic and electronic degrees of freedom.

*Electronic address: shlee@phy.cuhk.edu.hk
†Electronic address: jwan@phy.cuhk.edu.hk

Also, M_I and q_I represent the mass and charge of the Ith ion. The last term $E_{\rm KS}[\{\mathbf{R}_I\},\{\psi_n\}]$ is the Kohn-Sham energy functional of the ion-electron system. Within adiabatic approximation, $E_{\rm KS}[\{\mathbf{R}_I\},\{\psi_n\}]$ is given by DFT, and $E_{\rm KS}$ depends on the configuration of ions for bulk systems. The first and the second terms in Eq. (1) are the classical kinetic and coulomb energy of the ions. For a crystal system with small oscillation of ions, one can write $\mathbf{R}_I = \mathbf{R}_I^0 + \delta\mathbf{R}_I$, where $\mathbf{R}_I^0$ and $\delta\mathbf{R}_I$ are respectively the equilibrium position and the (small) displacement from $\mathbf{R}_I^0$ of the Ith ion. In addition, we can assume that each ion is under the influence of an effective local potential, given by $(1/2)K_{I,\alpha}(\delta R_{I,\alpha})^2$. Here $K_{I,\alpha}$ is the effective force constant, which includes the contributions from ion-ion and electron-ion interactions, and α is the component of displacement ($\alpha = 1,2,3$). As a result, the total internal energy [Eq. (1)] can be approximated by

$$\begin{aligned} U &\approx \Big\langle \sum_I \frac{1}{2} M_I \delta\dot{R}_I^2 \Big\rangle + \sum_{I,J\neq I} \frac{1}{2} \frac{q_I q_J}{|\mathbf{R}_I^0 - \mathbf{R}_J^0|} \\ &+ E_{\rm KS}[\{\mathbf{R}_I^0\},\{\psi_n^0\}] + \Big\langle \sum_{I,\alpha} \frac{1}{2} K_{I,\alpha}(\delta R_{I,\alpha})^2 \Big\rangle \\ &= \langle T\rangle + U_{\rm ion}^0 + E_{\rm KS}^0 + \langle \delta E\rangle, \end{aligned} \tag{2}$$

which could be understood as the sum of zero-temperature energies (quantities with superscript 0) and the contribution due to thermal motions of ions (quantities with $\langle\cdots\rangle$).

In first-principles calculations, $E_{\rm KS}^0$ and $\langle\delta E\rangle$ depend on the choice of XC functional, whereas $\langle T\rangle$ equals $3Nk_BT/2$ regardless of the choice of XC, because the ionic motions are treated classically. Therefore, Eq. (2) can be written as,

$$U = \frac{3}{2} N k_B T + \langle E\rangle, \tag{3}$$

where

$$\langle E\rangle = U_{\rm ion}^0 + E_{\rm KS}^0 + \langle\delta E\rangle, \tag{4}$$

is the total DFT energy of the system. We now consider the internal energy calculated by two different choices of XC, say XC_1 and XC_2, the difference between U is given by

$$\begin{aligned} \Delta U(V,T) &= U_{\mathrm{XC}_1}(V,T) - U_{\mathrm{XC}_2}(V,T) \\ &= \langle E_{\mathrm{XC}_1} - E_{\mathrm{XC}_2}\rangle. \end{aligned} \tag{5}$$

As $U_{\rm ion}^0$ only depends on the equilibrium ionic configuration, it does not contribute to $\Delta U(V,T)$. Moreover, $\langle\delta E\rangle$ should be equal to $3Nk_BT/2$, because $\delta R_{I,\alpha}$ is regarded as a classical degree of freedom and

$$\langle \frac{1}{2} K_{I,\alpha}(\delta R_{I,\alpha})^2\rangle = \frac{1}{2} k_B T,$$

at thermal equilibrium. Therefore, ΔU becomes

$$\Delta U(V,T) = E_{\mathrm{KS,XC}_1}^0 - E_{\mathrm{KS,XC}_2}^0, \tag{6}$$

which depends solely on the system volume. More importantly, the difference between the calculated pressures, given by

$$P_{\mathrm{XC}_1}(V,T) - P_{\mathrm{XC}_2}(V,T) = -\frac{\partial\langle E_{\mathrm{XC}_1} - E_{\mathrm{XC}_2}\rangle}{\partial V}\bigg|_S, \tag{7}$$

(where S represents the entropy of the system) should be, in general, a function of V and T. However, according to Eqs. (5) and (6), although both E_{XC_1} and E_{XC_2} depend on temperature, their difference, $E_{\mathrm{XC}_1} - E_{\mathrm{XC}_2}$ should not. Consequently, the resultant difference in pressure should also be temperature independent, that is,

$$P_{\mathrm{XC}_1}(V,T) - P_{\mathrm{XC}_2}(V,T) = \Delta P_{12}(V). \tag{8}$$

III. METHODOLOGY

To illustrate the relationships in Eqs. (6) and (8), we perform FP calculations on periclase MgO at thermodynamic conditions that range from ambient conditions to pressures and temperatures that are close to those of a deep Earth environment. Periclase MgO has a face-centered cubic structure and is known to be stable in the pressures and temperatures being considered in this work. Therefore, structural changes, such as phase transition and melting, are avoided.

The EOS at each temperature are determined by first-principles molecular dynamics simulations. For each simulation, the simulation supercell consists of 64 atoms (32 MgO units). These atoms were first arranged in a face-centered cubic (fcc) configuration, and the atomic trajectories and electronic orbitals were evolved via Car-Parrinello molecular dynamics (CPMD) [21], with the temperature controlled by the Nosé thermostat technique [22], at T = 300 K, 1000 K, 2000 K,... 4000 K, at various cell volumes. The calculations are repeated using both LDA and GGA exchange-correlations. The pressures determined at each temperature are fitted against the third-order Birch-Murnaghan EOS [23]. As a result, two EOSs at each temperature are obtained, one LDA and one GGA.

The choice of the XC energy functional is implemented in the generation of the pseudopotentials. In this study, two pairs of pseudopotentials for Mg and O are generated, one pair generated using LDA and the other using GGA. Apart from this difference in XC, all of the other parameters, such as the cutoff radius and the valence states, are the same. For Mg, a norm conserving pseudopotential [24] with nonlinear core correction [25] is used, whereas for O an ultrasoft [26] pseudopotential is used. The reference configuration is 3s1.5 3p0 3d0 for Mg and 2s2 2p2 for O. For CPMD, a fictitious electron mass μ_e = 400 m_e and a simulation time step of Δt = 12 atomic time units ($\sim$ 0.3 fs) are used. Electronic wavefunctions are expanded by planewaves with a cutoff of 30 Ry, and the cutoff for charge density is 240 Ry. To ensure enough statistical data, the simulations are run for more than 4 ps at each V, T point.

IV. RESULTS AND DISCUSSION

A. Equation of states and bulk modulus

The EOS given by our LDA and GGA calculations are shown in Fig. 1. The results are fitted against the third-order Birch-Murnaghan EOS, with $V_0 = 3782.30\ a_B^3$, $K_0 = 177.486$ GPa, and $K_0' = 4.026$ for LDA and $V_0 = 4046.43\ a_B^3$, $K_0 = 149.320$ GPa, and $K_0' = 4.080$ for GGA. To ensure that our calculations are compatible with existing results, we compare our results with those obtained by Karki et al. [27], and Isaak et al. [28]. The bulk moduli for each EOS are shown in Fig. 2. We recalculate the static EOS of Karki et al. [27] by using the same PP files as in their work [29], and the recalculated static EOS is in excellent agreement with their published EOS parameters. In addition, such EOS was shown to be highly consistent with the experimental measurements at moderate pressures ($P < 170$ GPa). Therefore, Fig. 1 and Fig. 2 illustrate the discrepancy that arises from different methodologies, such as the implementation of PP, the choice of XC functionals, and the interaction potentials.

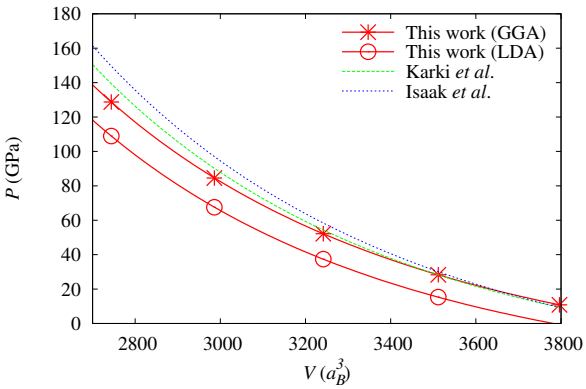

FIG. 1: (Color online) Calculated equations of state for MgO by LDA (circle) and GGA (star) at 0 K. The results of Karki et al. [27] (dashed line) and Isaak et al. [28] (dotted line) are given for comparison. The EOSs are drawn using the published EOS parameters.

At first glance, this discrepancy appears to reduce as the system volume increases. This is because both the pseudopotential errors and the difference between the XC functionals become less significant as atomic separation increases. Also, the GGA-calculated pressure and the bulk modulus in this work deviate systematically from those of LDA. In addition, our GGA results are more compatible with those estimated in Ref. 27 and Ref. 28 than our LDA calculations. This indicates that the GGA calculation should, in principle, be closer to the experimental measurements. The Mg PP used in Ref. 27 was optimized by using a combination of various electronic configurations, and a norm-conserving O PP was used. Nevertheless, the optimization of a PP configuration is the subject of further study. We concentrate on the errors introduced by the XC alone.

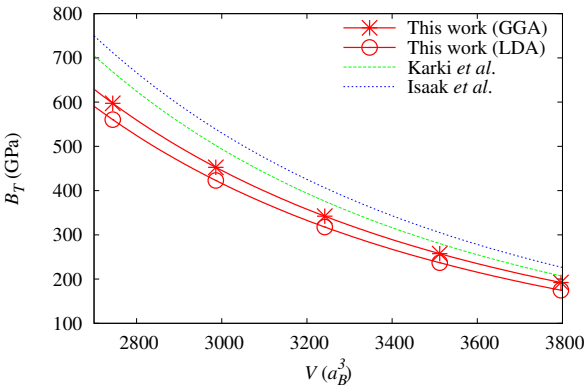

FIG. 2: (Color online) Isothermal bulk moduli given by various calculations.

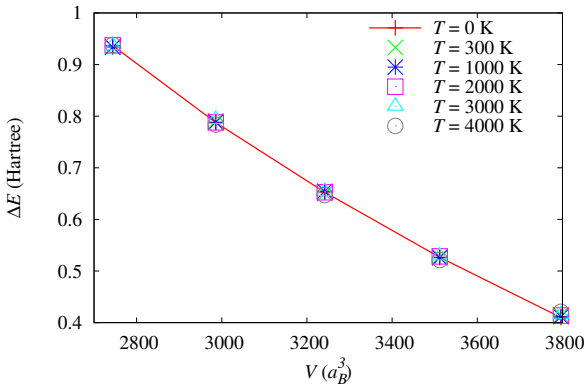

FIG. 3: (Color online) DFT total energy difference between GGA and LDA against volume at different temperatures. The results for $T = 0$ K are joined for visualization.

B. Energy and pressure differences

According to Eq. (5), it is intuitive to calculate the difference in energy at each temperature and volume. In Fig. 3, we plot the difference in energy, $\Delta E = E_{\rm GGA} - E_{\rm LDA}$, against V at each temperature and find that it does not depend on temperature. This is consistent with the prediction of Eq. (6). The differences between the pressures estimated by LDA and GGA at each temperature, $\Delta P = P_{\rm GGA} - P_{\rm LDA}$, are shown in Fig. 4. As can be seen, the differences in pressure at all temperatures almost coincide, with a maximum deviation of about 1 GPa, which is much smaller than the typical statistical error in pressure estimated by the DFT-based calculations. This is again in accordance with the conjecture of Eq. (8), and the pressure difference should be independent of temperature. Within the pressure range

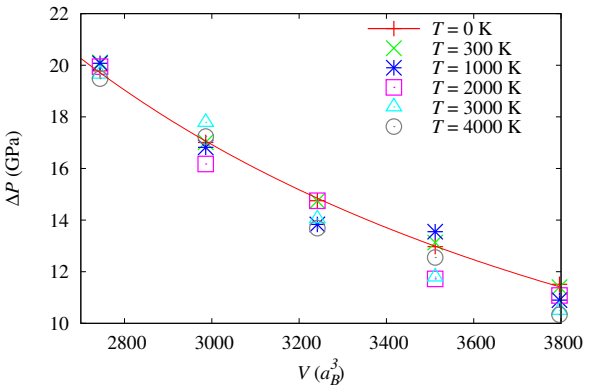

FIG. 4: (Color online) Difference in pressure $\Delta P = P_{\rm GGA} - P_{\rm LDA}$ at each temperature. Note that the pressure difference is in the order of 10 GPa, and the maximum difference between these points is about 1 GPa, which is negligible in DFT-based calculations. The pressure difference for $T = 0$ K is fitted against $\Delta P = a_1/V + a_2/V^2$ with $a_1 = 1.53 \times 10^4$ GPa a_B^3 and $a_2 = 1.06 \times 10^8$ GPa a_B^6 for visualization.

we have examined (0 GPa $< P <$ 170 GPa), $\Delta P(V)$ behaves asymptotically as a polynomial of $1/V$, that is,

$$\Delta P(V) \simeq \sum_{n=1}^{\infty} a_n \left(\frac{1}{V}\right)^n. \qquad (9)$$

Here, a few comments are in order. The present analysis implies that the thermodynamic quantities, such as internal energy and pressure, calculated by FP methodologies with a particular XC functional can easily be transformed into those obtained by another choice of XC functional. For example, the difference in heat capacity, given by

$$\begin{aligned} \Delta C_V &= C_{V,\rm GGA} - C_{V,\rm LDA} \\ &= \frac{\partial \langle E_{\rm GGA} - E_{\rm LDA} \rangle}{\partial T} = \frac{\partial \langle \Delta E \rangle}{\partial T} = 0, \end{aligned} \qquad (10)$$

at each volume should vanish because ΔE does not depend on temperature. This implies that the heat capacity calculated by any XC should be the same. In addition, the Grüneisen parameter,

$$\gamma = \frac{\alpha K_T V}{C_V}, \qquad (11)$$

calculated by different XC functionals should also be the same. Here $\alpha = (1/V)(\partial V/\partial T)_P$ and $K_T = -V(\partial P/\partial V)_T$ are, respectively, the coefficient of thermal expansion and the isothermal bulk modulus. To prove the statement, we consider the following thermodynamic relation,

$$\left(\frac{\partial P}{\partial T}\right)_V = -\left(\frac{\partial V}{\partial T}\right)_P \left(\frac{\partial P}{\partial V}\right)_T = \alpha K_T. \qquad (12)$$

Therefore, Eq. (11) can be written as

$$\gamma = \frac{V}{C_V}\frac{\partial P}{\partial T}. \qquad (13)$$

As a result, the difference in the Grüneisen parameter,

$$\begin{aligned} \Delta\gamma(V,T) &= \frac{V}{C_{V,\rm GGA}(V,T)}\frac{\partial P_{\rm GGA}(V,T)}{\partial T} \\ &- \frac{V}{C_{V,\rm LDA}(V,T)}\frac{\partial P_{\rm LDA}(V,T)}{\partial T} \\ &= \frac{V}{C_V(V,T)}\frac{\partial \Delta P(V,T)}{\partial T} = 0, \end{aligned} \qquad (14)$$

should vanish either.

The present estimation of pressure and energy differences is based on calculations of the cubic MgO structure. In principle, our analysis should be valid for any crystal system with small oscillation of ions, although the corresponding FP calculations may require extra care in the estimation of pressure. Although not shown in this work, our preliminary calculations on $MgSiO_3$ perovskite and post-perovskite phases [30] support our proposed theory. For a non-cubic crystal structure, a finite strain may introduce shear stress to the system. In such a case, the EOS should be determined by cell dynamics algorithms [4, 5]. It should also be noted that our conclusion on the pressure correction relies on the assumption that the thermal contribution to the total internal energy is governed by classical mechanics. However, this may not be valid in situations where quantum mechanical interactions, such as phonon vibration should be taken into account. In particular, at extremely low temperatures, long range acoustic phonon modes play an important role in various thermodynamic phenomena. Nevertheless, recent works on structural phase transition in $MgSiO_3$ at coremantle boundary conditions [31] and postspinel transition in Mg_2SiO_4 [32] have shown that high-temperature thermodynamic properties estimated by phonon-based calculations should not depend on the choice of XC functionals, as long as quasiharmonic approximation (QHA) remains valid in the thermodynamic conditions of interest. For example, different choices of XC functionals only affect the position of the estimated phase boundaries in these works but not the Clapeyron slopes. In addition, the recent theoretical study of ultrahigh-pressure EOS of MgO [33] has also shown explicitly that, within the QHA validity regime, the difference between a LDA-EOS and a GGA-EOS is independent of temperature. More importantly, it should be noted that QHA requires the vibrational amplitude of each atom to be small, which is the major assumption of our pressure correction conjecture. As a result, the work of Wu et al. [33] ubiquitously supports our hypothesis of pressure correction, even the FP methodologies used (lattice dynamics) in this work are different from ours (Car-Parrinello molecular dynamics).

The validity and behavior of $\Delta P(V)$ are also subjects for further investigation. In the pressure range we have

investigated, $\Delta P(V)$ is finite and is well approximated by Eq. (9), which implies that the pressure difference should increase with a decreasing volume. However, this is not valid either when V approaches infinity ($V \to \infty$) or when V becomes vanishingly small ($V \approx 0$). In the former case, the system consists of isolated atoms, and the energy difference that is due to different XC is constant; as a result $\Delta P(V)$ is zero as $V \to \infty$. In the latter case, the inter-atomic distance approaches zero, the interacting electrons should be well described by the free electron gas model, and LDA and GGA should give the same pressure. Last but not the least, the present study focuses on the pressure correction due to the chosen XC functional, which is in opposite to the idea of *volume correction* suggested by Wu et al. [33], in which an EOS is corrected to match experimental data. A combination of these EOS corrections will make various FP-based results more transferable, thus allowing one to have an effective recipe to transform the calculated thermodynamic quantities from one condition to another.

V. CONCLUSION

To conclude, by using MgO as a prototype system, we have studied the discrepancy in pressure that is due to different choices of XC functionals in DFT calculations. We have found that the differences in energy and pressure for GGA and LDA calculations should be independent of temperature. As a result, one may easily constrain the XC error at arbitrary temperatures. This may lead to a better estimation of thermodynamic properties, such as heat capacity and the Grüneisen parameter, in the systems that are being investigated by the FP and high-pressure communities.

ACKNOWLEDGEMENTS

The authors acknowledge help from S. C. Sung and a useful discussion with A. R. Oganov. S. H. Lee acknowledges the support of S. M. Wong and S. F. Tsang. Jones T. K. Wan acknowledges the support of S. S. Lam and T. L. Wan. First-principles calculations were performed using the Car-Parrinello molecular dynamics code in Quantum-ESPRESSO ver. 3.1.1. Computation was performed using the CUHK high-performance computing (HPC) facility. This work is supported by RGC-HK (CERG project no. 403007) and CUHK (direct grant no. 2060307) grants.

[1] P. Hohenberg and W. Kohn, Phys. Rev. **136**, B864 (1964).
[2] W. Kohn and L. J. Sham, Phys. Rev. **140**, A1133 (1965).
[3] M. P. Allen and D. J. Tildesley, eds., *Computer Simulation in Chemical Physics*, vol. 397 of *NATO Science Series C* (Springer, Berlin, 1993).
[4] R. M. Wentzcovitch, J. L. Martins, and G. D. Price, Phys. Rev. Lett. **70**, 3947 (1993).
[5] M. Parrinello and A. Rahman, Phys. Rev. Lett. **45**, 1196 (1980).
[6] R. Car, Quant. Struct.-Act. Relat. **21**, 97 (2002).
[7] P. Carloni, Quant. Struct.-Act. Relat. **21**, 166 (2002).
[8] A. R. Oganov, G. D. Price, and S. Scandolo, Z. Kristallogr. **220**, 531 (2005).
[9] P. E. Blöchl, Phys. Rev. B **50**, 17953 (1994).
[10] A. A. Mostofi, J. R. Yates, Y. S. Lee, I. Souza, D. Vanderbilt, and N. Marzari, Comput. Phys. Commun. **178**, 685 (2008).
[11] B. B. Karki, L. Stixrude, S. J. Clark, M. C. Warren, G. J. Ackland, and J. Crain, Am. Mineral. **82**, 635 (1997).
[12] B. B. Karki, R. M. Wentzcovitch, S. de Gironcoli, and S. Baroni, Phys. Rev. B **62**, 14750 (2000).
[13] A. R. Oganov, J. P. Brodholt, and G. D. Price, Earth Planet. Sci. Lett. **184**, 555 (2001).
[14] A. R. Oganov, J. P. Brodholt, and G. D. Price, Nature **411**, 934 (2001).
[15] L. Stixrude and B. Karki, Science **310**, 297 (2005).
[16] J. T. K. Wan, T. S. Duffy, S. Scandolo, and R. Car, J. Geophys. Res. **112**, B03208 (2007).
[17] J. P. Perdew, K. Burke, and M. Ernzerhof, Phys. Rev. Lett. **77**, 3865 (1996).
[18] D. M. Ceperley and B. J. Alder, Phys. Rev. Lett. **45**, 566 (1980).
[19] A. Yeganeh-Haeri, Phys. Earth Planet. Int. **87**, 111 (1994).
[20] N. L. Ross and R. M. Hazen, Phys. Chem. Miner. **16**, 415 (1989).
[21] R. Car and M. Parrinello, Phys. Rev. Lett. **55**, 2471 (1985).
[22] S. Nosé, Mol. Phys. **52**, 255 (1984).
[23] F. Birch, Phys. Rev. **71**, 809 (1947).
[24] N. Troullier and J. L. Martins, Phys. Rev. B **43**, 1993 (1991).
[25] S. G. Louie, S. Froyen, and M. L. Cohen, Phys. Rev. B **26**, 1738 (1982).
[26] D. Vanderbilt, Phys. Rev. B **41**, 7892 (1990).
[27] B. B. Karki, R. M. Wentzcovitch, S. de Gironcoli, and S. Baroni, Phys. Rev. B **61**, 8793 (2000).
[28] D. G. Isaak, R. E. Cohen, and M. J. Mehl, J. Geophys. Res. **95**, 7055 (1990).
[29] The pseudopotential files are available at www.pwscf.org.
[30] S. H. Lee, S. C. Sung, and J. T. K. Wan, private communications.
[31] T. Tsuchiya, J. Tsuchiya, K. Umemoto, and R. A. Wentzcovitch, Earth Planet. Sci. Lett. **224**, 241 (2004).
[32] Y. G. Yu, R. M. Wentzcovitch, T. Tsuchiya, K. Umemoto, and D. J. Weidner, Geophys. Res. Lett. **34**, L10306 (2007).
[33] Z. Wu, R. M. Wentzcovitch, K. Umemoto, B. Li, and K. Hirose, J. Geophys. Res. **113**, B06204 (2008).